

# Effect of Spark Plasma Sintering (SPS) at Temperatures of 900 and 950°C for 5 Minutes on Microstructural Formation of Fe-25Ni-17Cr Austenitic Stainless Steel

M. Dani<sup>1\*</sup>, S. Mustofa<sup>1</sup>, Parikin<sup>1</sup>, Sumaryo<sup>1</sup>, T. Sudiro<sup>2</sup>, B. Hermanto<sup>2</sup>, D. R. Adhika<sup>3,4</sup>, A. Insani<sup>1</sup>,  
A. Dimiyati<sup>1</sup>, Syahbuddin<sup>5</sup>, Sri Hardjanto<sup>6</sup>, E. A. Basuki<sup>7</sup>, C. A. Huang<sup>8</sup>

<sup>1</sup>Center for Sci. and Tech. of Adv. Materials, BATAN, Kawasan Puspiptek Serpong, South Tangerang 151314, Indonesia

<sup>2</sup>Research Center of Physics - LIPI, Kawasan Puspiptek Serpong, South Tangerang 15314, Indonesia

<sup>3</sup>Research Center for Nanosciences and Nanotechnology, Bandung Institute of Tech., Jl. Ganesha 10, Bandung 40132, Indonesia

<sup>4</sup>Adv. Functional Mat. Res. Group, Fac. of Industrial Tech., Bandung Institute of Tech., Jl. Ganesha 10, Bandung 40132, Indonesia

<sup>5</sup>Dept. of Mechanical Eng., Fac. of Eng., Pancasila University, Srengseng Sawah, Jagakarsa, South Jakarta 12640, Indonesia

<sup>6</sup>Dept. of Metallurgy and Materials Eng., Fac. of Eng., University of Indonesia

<sup>7</sup>Dept. of Metallurgical Eng., Bandung Institute of Tech., Jl. Ganesha 10, Bandung 40132, Indonesia

<sup>8</sup>Dept. of Mechanical Engineering, Chang Gung University, Taoyuan, Taiwan

\* Corresponding author: mdani6770@gmail.com

## ABSTRACT

*Purpose:* This research is related to fabricate Fe-25Ni-17Cr austenitic stainless steel.

*Methodology:* Fe-25Ni-17Cr austenitic stainless steel were made by spark plasma sintering at 900 and 950°C for 5 minutes.

*Results:* The microstructure of both the steels sintered at 900 and 950°C consists of particles with high Cr content, a'-Cr and austenite matrix containing of fine grains of g-FeNi. Sintering at high temperatures causes the fine grains to be seen more clearly. The fine grains of g-FeNi are twin grains that contain defects such as dislocations, stacking faults and trapped air bubbles. The defects are formed during the mixing process through milling and compacting under a 30 MPa load during the sintering process. The density of the first two defects decreased with increasing the sintering temperature. By contrast, more trapped air bubbles were noticed as increasing the sintering temperature and the distribution of fine a'-Fe particles higher. Since beside of higher the density of steel sintered at the high temperature, smaller grain size of austenite matrix and higher distribution of fine a'-Fe in the austenite matrix, the hardness of this steel is greater than the steel sintered at temperature of 900°C.

*Applications/Originality/Value:* This study fabricated austenitic stainless steel made from powders of 58% Fe, 25% Ni and 17% Cr. The manufacturing process is carried out through a sintering by spark plasma at temperatures of 900 and 950°C for 5 minutes. The microstructure of austenitic stainless steel that formed very well at 950°C consisted of very

fine grains of austenite g-FeNi and a'-Fe particles were distributed throughout the g-FeNi grains, resulting in a high hardness of 399.3 HV<sub>0.2</sub>.

**Key words :** Fe-25Ni-17Cr austenitic stainless steel, Spark Plasma Sintering, Microstructure, HRPD, SEM, TEM

## 1. INTRODUCTION

Austenitic stainless steel (ASS) is a type of steel containing the basic main elements of Cr  $\geq$  18.0% and Ni  $\geq$  8.0%, and small amounts of some addition elements such as Mo, Mn, Si, Ti, Nb, V, W, Cu, and Al [1]-[4]. This type of steel has offered great performance in strength, corrosion and creep resistances at high temperatures. Therefore, this steel is used for high temperature components of jet engines, power plants and nuclear reactors. In general, the stainless steel has been widely developed as wrought and casting products [5]-[7]. Wrought products are found in the form of sheets, bars, pipes and profiles that need an additional process such as forming, joining, machining, finishing to become the final product. Certain parts such as joints, the results of forming and machining of this final product certainly have many imperfections and are critical parts that need a lot of attention. While the cast product is formed by pouring liquid metal into a mould, then cooled and the shape of the product is almost close to its final dimension. Unfortunately, the mechanical properties of cast products are lower than wrought products due to porosity and inhomogeneity of the cast products. For this reason, many manufacturing methods have been developed including powder metallurgy for stainless steels [8]. However, the process takes longer time, results low

density and there is still porosity which decreases its mechanical properties. More recently this technology has been developed again and more promising such as very fast forming time, more homogeneous, high density and low porosity [9,10]. The process used for the powder metallurgy is known as Plasma Spark Sintering (SPS).

Along with the times, several stainless steels have been developed using the method of powder metallurgy through the process of sintering. The stainless steels of 316L series added MoSi<sub>2</sub> [11] and milling ball processes followed by sintering [12] have been carried out to increase density, obtain fine grains, improve mechanical properties, and corrosion resistance. Nickel-free steel powder containing nitrogen was processed by spark plasma sintering to determine the effect of sintering temperature [13]. The influence of temperature was on the density of the alloy, microstructure and hardness of the steel. Likewise, a successful study characterized microstructure and mechanical reinforcement of 15Cr ODS steel produced by mechanical integration and spark plasma sintering [14]. Little has been done on the manufacture of austenitic stainless steels with high Ni content by metallurgical powder through a process of spark plasma sintering. Therefore, this study tries to develop austenitic stainless steels with a composition of 58% Fe, 17% Cr, and 25% Ni powders through the process of plasma spark sintering. The sintering process temperatures were set at 900 and 950°C for 5 minutes. Through testing with equipment of high-resolution neutron diffractometers (HRND), optical microscope (OM), scanning (SEM) and transmission electron microscope (TEM) mounted energy dispersed spectrometers (EDS) as well as micro hardness tests, microstructure, main structures formed as matrix, second phases, particles and hardness of Fe-25Ni-17CrASS are investigated in the study.

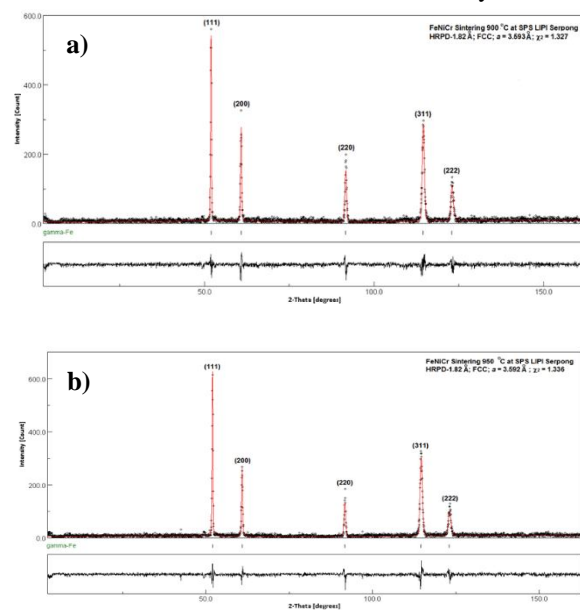
## 2. EXPERIMENTAL PROCEDURE

The materials used in this study was high purity metal powder of Fe, Ni and Cr. The element contents in the austenitic stainless steel in% by weight were 58.00%, 25.00% and 17.00% respectively. The following element contents mentioned in this study is stated in% by weight. The three powder ingredients were mixed through a milling device for 5 hours. The results of the mixing were compacted by a compacting process under a load of 30 MPa to form a coin of about 15 mm in diameter and 2.5 mm thick and sintered at temperatures of 900 and 950°C for 5 minutes in an SPS Fuji-625 (Fuji Electronic Industrial Co., Ltd.), crystal structure of the matrix for the Fe-25Ni-17Cr ASS was determined through a high-resolution neutron diffractometer (HRND) in the Siwabessy nuclear reactor, Puspipstek Region, Serpong, Indonesia. For observing the microstructure of steel, the coin was prepared through a standard metallurgical process which includes grinding on SiC sandpapers from rough grid size of 200 Si to fine grid size of 5000. Then it was polished with a paste containing diamond particles of a maximum size of 1 mm and then etched to reveal the

microstructure of the Fe-25Ni-17Cr ASS. The microstructure of Fe-25Ni-17Cr ASS was observed through an optical microscope (OM), a scanning electron microscope (SEM) of JSM-7600F (Jeol Ltd., Tokyo, Japan) which was operated at a voltage of 20 kV and a transmission electron microscope (TEM) of Hitachi H-9500 operated at a voltage of 300 kV. The devices are completed by a energy dispersive spectrometer (EDS) in order to determine the composition of phases formed in the Fe-25Ni-17CrASS. In addition, TEM samples were prepared by micro sampling method on focused ion beam (FIB) Hitachi FB-2200 at an operating voltage of 40 kV.

## 3. RESULTS

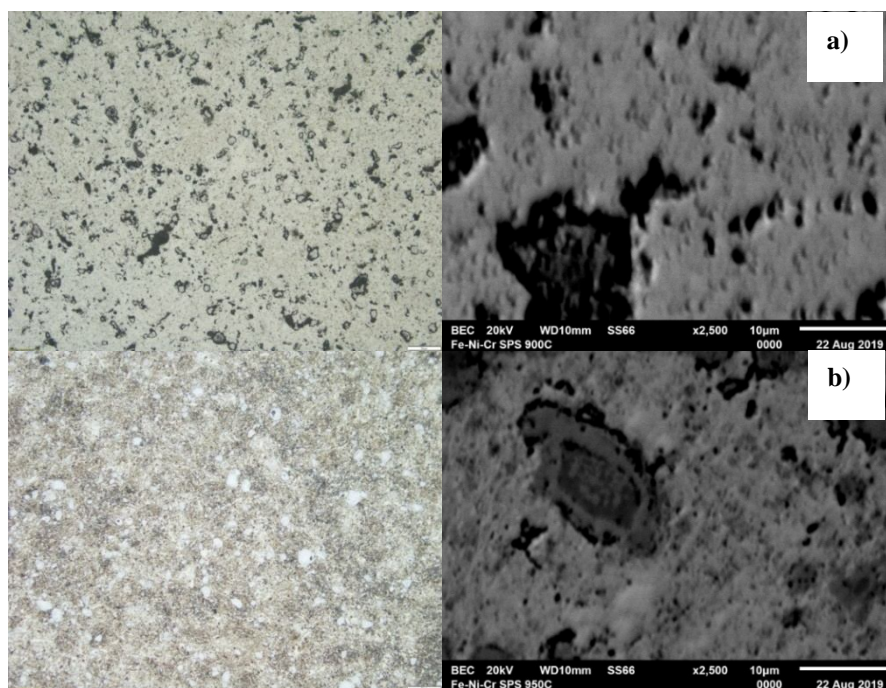
By a capability to penetrate the sample much deeper to several centimeters, a high-resolution neutron diffractometer (HRND) located in the Siwabessy reactor, Serpong, the Puspipstek region was used in this study. Similar to X-ray diffraction patterns [15], some prominent peaks associated with planes of (111), (200), (220), (311), (222) and (331) are also presented in neutron diffraction patterns as shown in Figure 1 a) and b). Using the Rietveld refinement method for removing back noises in the diffraction patterns, lattice parameters, *a*, face-centered cubic structure of Fe-25Ni-17Cr austenitic stainless steel sintered at 900°C for 5 minutes was determined about 3.593 Å. The lattice parameter of the crystal structure formed on Fe-25Ni-17Cr austenitic stainless steel after sintered at 950°C for 5 minutes was 3.592 Å. Both patterns also have sharp peaks, which indicates that crystals are formed perfectly in the austenite matrix of Fe-25Ni-17Cr ASS. Some studies about austenitic stainless steels and superalloys [15-18] have reported the lattice parameters of austenite matrix close to the results of this study.



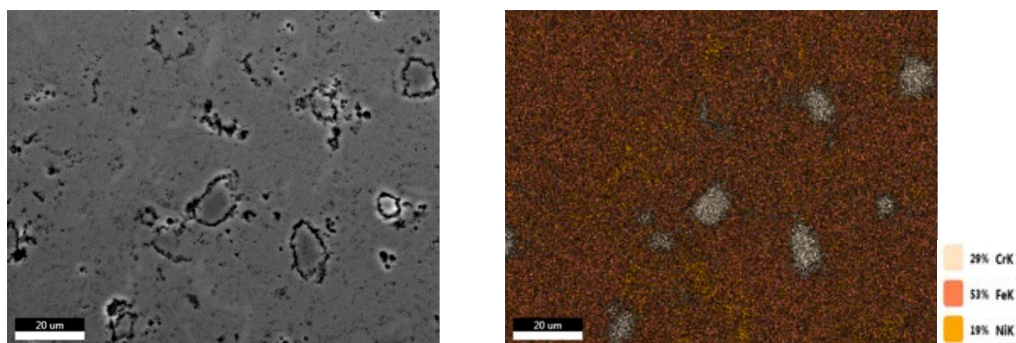
**Figure 1:** High resolution neutron diffraction patterns that have been refined by the Rietveld refinement method for Fe-25Ni-17Cr ASS formed after spark plasma sintering a) 900 and b) 950°C for 5 minutes

Sintering using SPS on the Fe-17Cr-25Ni ASS formed particles with a distribution as shown in Figure 2.a for temperature of 900°C and Figure 2.b for temperature of 950°C. Higher temperature makes the particles develop faster and larger in number more than after sintering at a temperature of 900°C especially in the particle size < 1 μm, as reported by S. Mustofa *et al.* [15]. The larger particle size in the austenite matrix can reach 10 μm both after sintering at 900 and 950°C for 5 minutes. However, a thin layer has been formed on the particles after sintering at 950°C, whereas the particles after being sintered 900°C is in a plain state. Although two samples with austenite matrix are arranged by perfect crystals as shown by the results of XRD [15] and

neutron diffraction analysis, fine grains in matrix those produced at 950°C sintering can be seen clearer. In Figure 3, it can be seen the distribution of constituent elements, namely Cr, Fe and Ni on the microstructure of Fe-25Ni-17Cr austenitic stainless steel resulting from sintering at temperatures of 900 and 950°C for 5 minutes. Although the surface of microstructure sintered at 950°C looks rougher than the surface of the sintered 900°C, the content of elements such as Cr, Fe and Ni is almost the same in both alloys. The particles formed are dominated by high Cr content, whereas Fe and Ni are spread evenly which is thought to form g-FeNi compounds as austenitic matrix Fe-25Ni-17Cr austenitic stainless steel sintered 900°C as identified through high-resolution neutron diffractions.



**Figure 2:** Optical and SEM micrographs displaying the microstructure of Fe-25Ni-17Cr ASS formed after spark sintering a) 900 and b) 950°C for 5 minutes



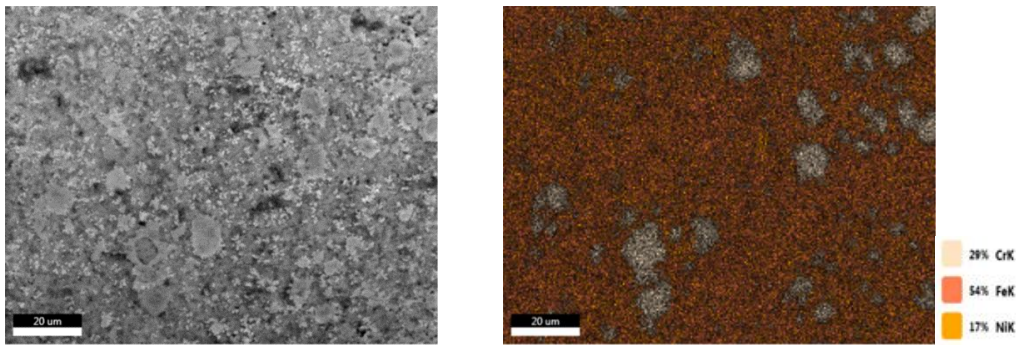


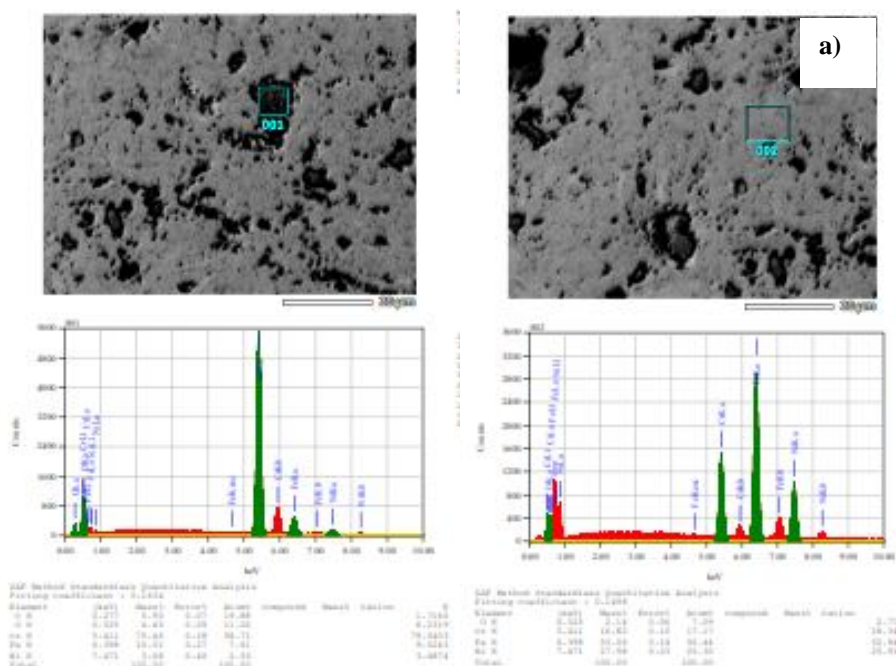
**Figure 3:** Element mapping in the microstructure of Fe-25Ni-17Cr- ASS formed after spark plasma sintering a) 900 and b) 950°C for 5 minutes

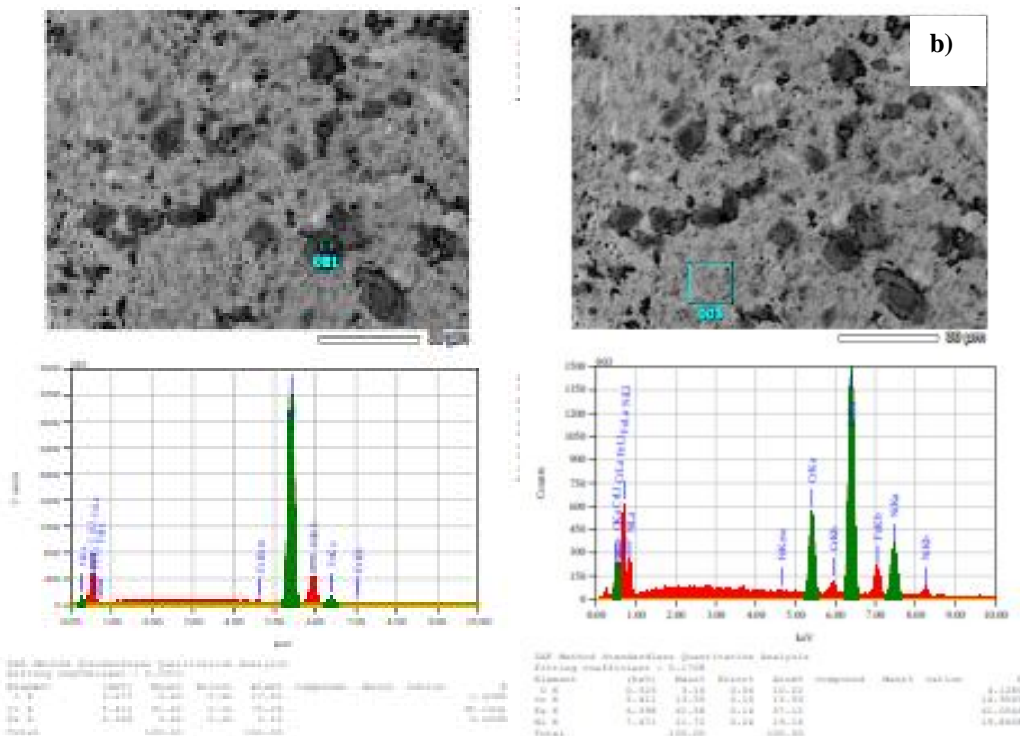
The same structure was also seen in the Fe-25Ni-17CrASS after sintering at 950°C. However, the austenite matrix composed by fine grains of g-FeNi is slightly visible on Fe-17Cr-25Ni ASS. Likewise, the boundary between the grains in this alloy has also been seen. Therefore, the influence of sintered temperature accelerates the formation of grains on the Fe-25Ni-17CrASS.

As shown in Figure 4 a) and b) that showing SEM micrographs and their EDS results, the particles formed in the austenite matrix contain high Cr which varies from 65.62 to 91.45%. By contrast, the Ni content in the particles is below 4.00% in both the Fe-25Ni-17Cr ASS after sintering at 900 and 950°C. The rest element in these particles is the Fe content. Therefore, it can be considered that the particles with high Cr content has a'-Cr phase. Furthermore, the austenitic matrix of Fe-25Ni-17Cr ASS formed after sintering 900 (a) and 950°C (b) each contained 2.19% O, 16.68% Cr, 51.93% Fe, 29.21% Ni and 3.16% O, 13.55% Cr, 61.58% Fe, 21.72% Ni. Both the composition of the matrix shows as g-FeNi.

Thus, the two Fe-25Ni-17Cr ASS consist of a'-Cr particles which are spread throughout the g-FeNi matrix.

Grains are more clearly visible through TEM images in Figure 5. Grains in the austenite matrix of the two steels sintered at temperatures of 900 and 950°C for 5 minutes are twin grains containing defects such as dislocation lines and trapped air bubbles. The density of dislocation is higher the grains of Fe-25Ni-17Cr ASS sintered at 900°C. Some stacking faults and trapped air bubbles are also found. Sintering at 950°C leads to decrease the density of dislocation and stacking faults, followed by increasing the number of trapped air bubbles. Using an intercept method, it has been determined that grain sizes have average diameters about 511.27 and 217.27 nm as in the austenite matrix of Fe-25Ni-17Cr ASS sintered at 900 and 950°C, respectively for 5 minutes. Higher temperature sintering decreases the density of dislocations and stacking fault and the grain size of austenite matrix. It increases distribution of a'-Fe particles and trapped air bubbles in the austenite matrix.

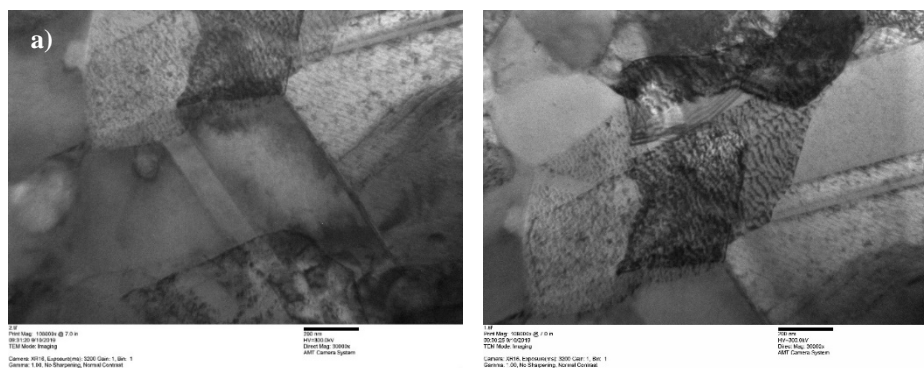




**Figure 4:** SEM micrographs and EDS results derived from the particles and matrices of Fe-25Ni-17Cr ASS formed after spark plasma sintering at a) 900 and b) 950°C for 5 minutes

As shown in the previous diffraction pattern, electron diffraction obtained from a fine grain with zone axis (013) was succeeded in determining the same structure as the austenite g-FeNi structure, i.e. face centered cubic. Through the diffraction points associated with the planes of face-centered cubic, the lattice parameter of the crystal structure of the Fe-25Ni-17Cr ASS sintered 900°C was determined to be  $a = 3.5526 \pm 0.0297 \text{ \AA}$ . The results obtained from particles sintered at the same temperature through the zone axis (021), found a body-centered cubic crystal structure with a lattice parameter to be  $a = 2.8694 \pm 0.0025 \text{ \AA}$ . This value for the matrix Fe-25N-17Cr ASS differs from the result of high-resolution neutron diffractions. The difference is due to the object for electron diffraction generated from a very small selected area on the sample that only contains one grain with a single crystal orientation on the area, while the neutron diffractions were obtained from a larger area that contains a lot of grains with different crystal orientations.

Likewise, the composition and crystal structure of phases formed in Fe-25Ni-17Cr ASS, through high-resolution observations of particles with high Cr content and grains of austenite matrix g-FeNi and electron diffraction patterns were successfully observed using TEM attached EDS. The composition of particle identified only had an elemental content of Cr of 38.72% and Fe of 61.28%. Likewise, the composition and crystal structure of phases formed in Fe-25Ni-17Cr ASS, through high-resolution observations of particles with high Cr content and grains of austenite matrix g-FeNi and electron diffraction patterns were successfully observed using TEM attached EDS. The composition of particle identified only had an elemental content of Cr of 38.72% and Fe of 61.28%. No Ni content can be detected in these particles. In addition, a grain in the austenite matrix was identified to have 30.76% Cr, 53.20% Fe and 16.04% Ni.



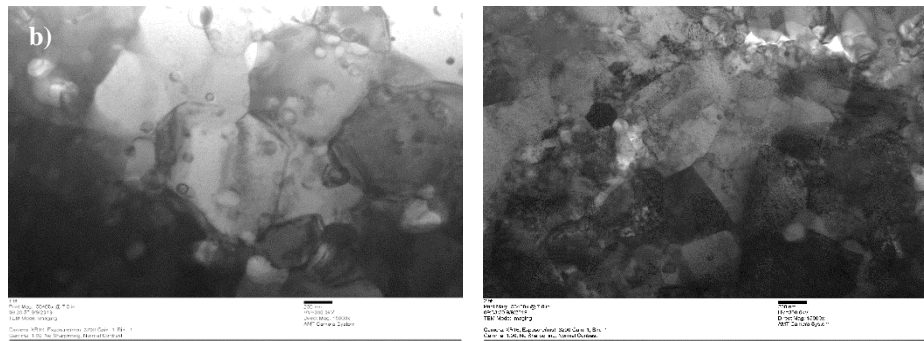
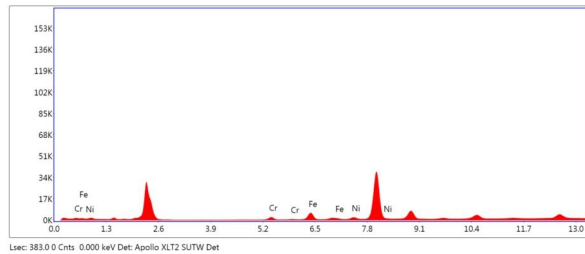
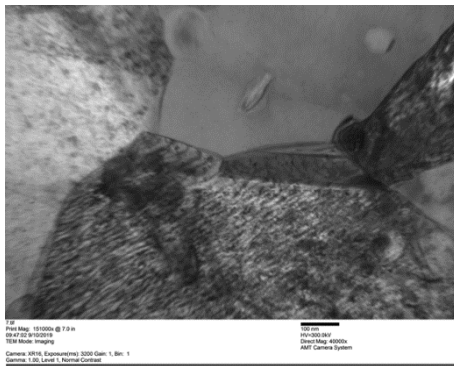


**Figure 5:** TEM bright field images of the Fe-25Ni-17CrASS formed after spark plasma sintering at a) 900 and b) 950°C for 5 minutes

Furthermore, the electron diffraction patterns of the two phases give results that show the crystal structure of body-centered cubic for the particle and face-centered cubic for the matrix. The chemical composition of the particles and

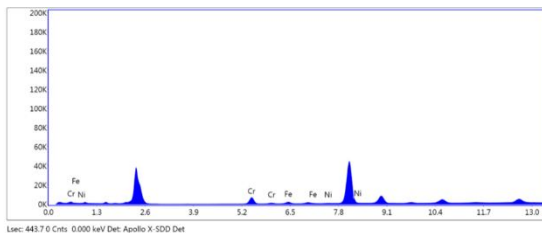
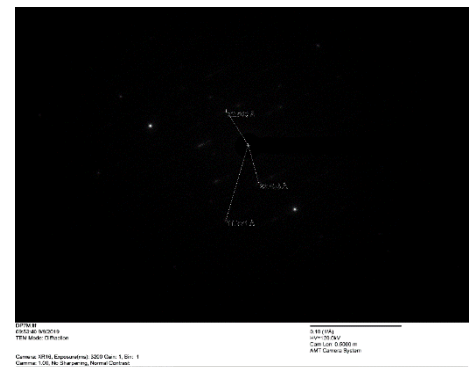
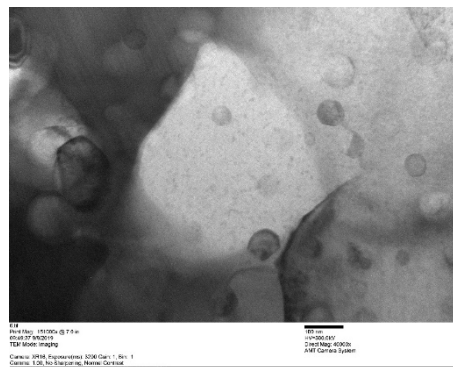
matrix are consistent with particles containing high Cr and austenite grains of g-FeNi making up the Fe-25Ni-17Cr matrix that were observed via SEM installed with EDS and HRPD.

### 3.1 Matrix



Element	Weight %	Atomic %	Net Int.	Net Error%	KABFactor
CrK	20.92	22.29	107.60	0.70	0.94
FeK	62.98	62.50	304.80	0.36	1
NiK	16.10	15.20	73.50	1.17	1.06

a) Matrix of g-FeNi



Element	Weight %	Atomic %	Net Int.	Net Error%	KABFactor
CrK	77.37	78.60	254.20	0.35	1
FeK	22.63	21.40	70.00	0.97	1.06
NiK	0.00	0.00	0.00	0.00	1.13

b) Particles of a'-Cr

**Gambar 6:** EDS results and electron diffraction generated from a) matrix g-FeNi and b) particle a'-Cr in the samples formed after SPS at 900 and 950°C for 5 minutes, respectively.

### 3.2 Mechanical Properties

As shown in Table 1, there are variations in the hardness of samples, both after sintering at 900 and 950°C. The hardness range of the 900°C sintered is between 283-310 HV<sub>0.2</sub>, while in the case of 950°C has a range between 379-420 HV<sub>0.2</sub>. Thus the average hardness of the Fe-25Ni-17Cr ASS sintered result at 900°C, which is  $295.5 \pm 11.3$  HV<sub>0.2</sub> lower than the average hardness of the sintered FeS-25Ni-17Cr ASS at 950°C, which is  $399.3 \pm 16.0$  HV<sub>0.2</sub>. The value is consistent with the results of previous studies which results in increasing the hardness as increasing the sintering temperature.

**Table 1:** Hardness of the Fe-25Ni-17Cr ASS after SPS at 900 and 950°C for 5 minutes

No.	Hardness (HV <sub>0.2</sub> )	
	Fe-25Ni-17Cr (900°C)	Fe-25Ni-17Cr (950°C)
1	298	399
2	283	379
3	278	391
4	304	420
5	294	374
6	304	409
7	310	388
8	308	420
9	283	404
10	293	409
<b>Ave.</b>	295.5	399.3
<b>Dev. Std.</b>	11.3	16.0

### 4. DISCUSSION

As discussed earlier, neutron diffraction patterns displaying prominent peaks corresponded to the same planes of a crystal structure of face-centered cubic formed in the Fe-25Ni-17Cr ASS after sintering at 900 and 950°C for 5 minutes. The face-centered cubic is included in the Fm4m space group and considered as austenite phase. The prominent peaks also found very sharp in both the diffraction patterns, indicating the both ASS having perfect crystals. Since no other peaks associated with other phases are seen in the two diffraction patterns, both the Fe-25Ni-17Cr ASS sintered at different temperatures has the austenite matrix of g-FeNi.

The microstructure of the two ASS consists of particles with high Cr content or 'Cr' phase which are distributed evenly on the austenite matrix of g-FeNi. Such structure is possible because the three constituent elements that are sintered to form the Fe-25Ni-17Cr ASS have different melting points. The melting point of Cr element is much higher compared to the melting point of Ni and Fe. Since in the process of sintering the diffusion process occurs between the particles of these elements, the tendency of diffusion between Ni and Fe is higher to form the austenite phase of g-FeNi and the diffusion between Fe and Cr is very small to form the a'-Cr phase. Therefore, the dominant structure of the Fe-25Ni-17Cr ASS is composed by austenite grains of g-FeNi and a'-Cr particles

are found spreading in the austenite grains of g-FeNi included its grain boundary. Increasing sintering temperature from 900 to 950°C does not significantly affect the austenite matrix of g-FeNi but it changes the particles to have thin film, showing diffusion process between Fe and Cr as seen in the figure 3. Moreover, the increasing sintering temperature accelerate the Cr atoms to assemble to be very fine particles so that the distribution of a'-Fe particles is more dispersed in the austenite matrix of g-FeNi formed at sintering temperatures at 950°C.

In the TEM image in the figure 6, the austenite matrix of Fe-25Ni-17Cr ASS after sintering has a twin structure. This is a characteristic of the structure of austenite g-FeNi grains. These results are consistent with several studies of the powder of 316 austenitic stainless steel that are formed by sintering processes including spark plasma sintering [12,19]. In addition, some crystal defects such as dislocations, and stacking faults formed during mixing in the milling process for 5 hours and compaction with a large load of 25 tons in the spark plasma sintering process are still noticed in the grains of Fe-25Ni-17Cr ASS. The density of dislocation and stacking faults decreased in the austenite grains sintered at 950°C. By contrast, the number of trapped air bubbles appear to increase with increasing sintering temperatures. This change is related to the dislocation reaction with the environment during sintering and new crystals largely nucleate during the recovery process of Fe-25Ni17Cr ASS which is deformed in the milling and compacting process. In addition, the particles that come in contact begin to bind to each other known as the neck region. High sintering temperatures accelerate the process of forming new crystals from dislocation and stacking faults defects compared to reducing these defects. In addition, the acceleration of the formation of new crystals at high sintering temperatures makes more air bubbles trapped. Because sintering at temperatures at 900°C seems to only make the diffusion process between powder particles bind to one another to form austenite matrix with density defects such as dislocations, stacking faults remains high and sintering at 950°C is able to change defects as nuclei new crystals for austenite grains of g-FeNi and make Cr atoms arrange themselves to form very fine sized a'-Cr particles.

Although the number of defects such as dislocation and stacking faults found in the Fe-25Ni-17Cr ASS after sintering at 950°C decreased, the hardness of ASS sintered at high temperatures was higher than the hardness resulting from sintering at low temperatures. This increase is related to an increase in the number of very fine particles (< 1 μm) of a'-Cr. This condition was followed by increasing the number of very fine grains of austenite g-FeNi. Moreover, the density of ASS produced from sintering at 900 and 950°C, respectively 7.38 and 7.42. The relative density of ASS at 950°C sintering is higher than 900°C, about 99.43%. A study [20] about W-Ni-Mn alloy formed through mechanical milling-assisted spark plasma sintering shows similar results.

Increasing sintering temperature from 1000 to 1150°C increased the mass density of the alloy. Increasing the sintering temperature from 800 to 1000°C also increased the density of nickel-free stainless-steel powder [13]. Therefore, increasing the hardness of AS15 Fe15Ni15Cr after sintering at high temperatures not only comes from defect density but is caused by an increase in the number of very fine particles of a'-Cr which may be in a critical size to increase mechanical strength, mass density and recrystallization formed fine grain in the matrix.

Further reading on related research in different applications such as [21], [22] and [23] can improve the integration of the research.

## 5. CONCLUSION

Process of spark plasma sintering at temperature of 900 and 950°C for 5 minutes to consolidate the Fe-25Ni-17Cr austenite stainless steel in this study can be concluded as follows: the matrix of Fe-25Ni-17Cr austenite stainless steel has austenite phase with the crystal structure of face centered cubic which is in Fm4m space group, the microstructure of Fe-25Ni-17Cr ASS consists of particles containing high Cr, known as a'-Cr and austenite matrix of g-FeNi, increasing the sintering temperature from 900 to 950°C leads the austenite grains with twin structure more finer, the density of dislocation and stacking faults are found to be the dominant defects in grains formed after sintering at 900°C which decreases with increasing sintering temperatures to 950°C, followed by increased trapped air bubbles, and much very fine particles of a'-Cr, large surface area of fine grains of g-FeNi and high mass densities which formed after sintering at a temperature of 950°C causes Fe-25Ni-17Cr ASS to have high hardness.

## ACKNOWLEDGEMENT

The authors would like to express our appreciation to the Head of the Center for Science and Technology for Advanced Materials, Prof. Dr. Ridwan, Head of PSTBM, Dr. Abu Khalid Rivai and Head of BTBM, Dr. Eng., Iwan Sumirat for their excellent support and coordinator so that this research can be finished properly. Financial support for this research was granted by Insinas Project No. No. 06/INS-1/PPK/E4/2019.

## REFERENCES

1. M. F. McGuire. *Stainless Steels for Design Engineers*, Ohio: ASM International, 2008, pp. 69-90.
2. R. L. Plaud, C. Herrera, and D. M. Escriba. **Short Review on Wrough Stainless Steels at High Temperatures: Processing, Microstructure, Properties and Performance.** *Materials Research*, vol. 10, no. 4, pp. 453-460, 2007.
3. A. F. Padilha and P.R. Rios. **Decomposition of Austenite in Austenitic Stainless Steels**, *ISIJ International*, vol. 42, no. 4, pp. 325-337, 2002.
4. T. Sourmail. **Precipitation in Creep Resistance Austenitic Stainless Steels**, *Materials Science and Technology*, vol. 17, pp. 1-15, 2007.  
<https://doi.org/10.1179/026708301101508972>
5. E. O. Yape. **Fe-Ni-Cr Crude Alloy Production from Direct Smelting of Chromite and Laterite Ores**, *Journal of Medical and Bioengineering*, vol. 3, no. 4, pp. 245-250, 2014.
6. Y. Liu, X. Lv, and C. Bai. **Evaluation Model for Viscosity of Fe-Ni-Cr Alloys Using Gibbs Free Energy of Mixing and Geometric Methods**, *ISIJ International*, vol. 57, no. 8, pp.1296-1302, 2017.
7. H. J. French, W. Kahlbaum, and A. A. Peterson. **Flow Characteristics of Special Fe-Ni-Cr Alloys and Some Steels at Elevated Temperatures**, *Bureau of Standards Journal of Research*, vol. 5, pp. 125-183, 1930.
8. E. Klar, P. K. Samal. **Power Metallurgy Stainless Steels: Processing**, Microstructure and Properties, ASM international, 2007.
9. P. Cavaliere. (Ed.). *Spark Plasma Sintering of Materials: Advances in Processing and Applications*, Switzerland: Springer International Publishing AG, 2019.
10. E. A. Olevsky and D. V. Dudina. *Field-Assisted Sintering: Science and Applications*, Switzerland: Springer International Publishing AG, 2018.
11. F. Akhtar, L. Ali, F. Peizhong, J. A. Shah. **Enhanced sintering, microstructure evolution and mechanical properties of 316L stainless steel with MoSi2 addition**, *Journal of Alloy and Compounds*, vol. 509, no. 35, pp. 8798-8797, 2011.
12. C. Keller, K. Tabalaiev, G. Marnier, J. Noudem, X. Sauvage, E. Hung. **Influence of Spark Plasma Sintering Condition on the Sintering and Functional Properties of an Ultra-fine Grains 316L Stainless Steel Obtained from Ball-milled Powder**, *Materials Science & Engineering A*, vol. 665, pp. 125-134, 2016.
13. Z. Xu, C. Jia, C. Kuang, K. Chu, X. Qu. **Spark Plasma Sintering of Nitrogen-containing Nickel-free Stainless Steel Power and Effect of Sintering Temperature**, *Journal of Alloys and Compounds*, vol. 484, pp. 924-928, 2009.
14. W. Li, H. Xu, X. Sha, J. Meng, W. Wang, C. Kang. **Microstructural Characterization and Strengthening Mechanism of a 15Cr ODS Steel Produced by Mechanical Alloying and Spark Plasma Sintering**, *Fusion Engineering and Design*, vol. 137, pp. 71-78, 2018.  
<https://doi.org/10.1016/j.fusengdes.2018.08.020>
15. S. Mustofa, M. Dani, Parikin et al. **Effect of Temperature of Spark Plasma Sintering on the Development of Oxide Compound in**

- Fe-25wt%Ni-17wt%Cr Austenitic Stainless Steel**, 2019.
16. M. Dani, A. Dimiyati, Parikin, J. G. Lesmana, A. K. Yahya, A. Insani, Syahbuddin, and C. A. Huang. **Microstructure of Austenitic Stainless Steel (25Ni17Cr) Solid Treated with Different Cooling Rate**, *International Journal of Technology*, 2019 (to be published).
  17. B. Geddes, H. Leon, and X. Huang. *Superalloy: Alloying and Performance*, Ohio: ASM International, 2010.
  18. C. W. Hong, Y. U. Heo, N. H. Heo, and S. J. Kim. **Coherent to incoherent transition of precipitates during rupture test in TP347H austenitic stainless steels**. *Materials Characterization*, vol. 115, pp. 71-82, 2016
  19. T. H. Kang, Y. K. Kim, M. H. Park, and K. A. Lee. **Room Temperature Compressive Properly and Deformation Behavior of Microporous STS 316L Stainless Steel Tube Manufacture with Powder Sintering Process**, *Journal of Nanoscience and Nanotechnology*, vol. 19, pp. 4015-4019, 2019.
  20. Y. Pan, D. Xiang, N. Wang, H. Li, and Z. Fan. **Mechanical Milling-Assisted Spark Plasma Sintering of Fine-Grained W-Ni-Mn Alloy**, *Materials*, vol. 11, p. 1323, 2018.
  21. Iasechko, M., Larin, V., Maksiuta, D., (...), Zinchenko, A., Vozniak, R. **Model description of the modified solid state plasma material for electromagnetic radiation protection**, *International Journal of Emerging Trends in Engineering Research* 7(10), pp. 376-382, 2019.  
<https://doi.org/10.30534/ijeter/2019/027102019>
  22. Turinskyi, O., Iasechko, M., Larin, V., (...), Tarshyn, V., Dziubenko, Y. **The investigation of the impulse evolution of the radio-frequency and optical radiation during the interaction with the solid-state plasma media on radioisotope and hexaferrite inclusions**, *International Journal of Emerging Trends in Engineering Research* 8(2),47, pp. 568-573, 2020.
  23. Darmawan, A.S., Siswanto, W.A., Sujitno, T. **Comparison of commercially pure titanium surface hardness improvement by plasma nitrocarburizing and ion implantation**, *Advanced Materials Research*, 789, pp. 347-351, 2013.